Antioxidant Properties of Biodiesel-Diesel Blends and Non-Isothermal Kinetic Studies of Schiff-Based Isatin-Thiosemicarbazone Derivatives

Nalan Turkoz Karakullukcu * , HALIL MUGLU , HASAN YAKAN , Volkan Murat YILMAZ , İkbal Agah İNCE

Posted Date: 3 June 2024

doi: 10.20944/preprints202406.0056.v1

Keywords: thiosemicarbazones; biodiesel; oxidative stability; kinetic study; energy

Article

Antioxidant Properties of Biodiesel-Diesel Blends and Non-Isothermal Kinetic Studies of Schiff-Based Isatin-Thiosemicarbazone Derivatives

Nalan Turkoz Karakullukcu [1,*], Halit Muglu [2], Hasan Yakan [3], Volkan Murat Yilmaz [4] and Ikbal Agah Ince [5,6]

[1] Blacksea Advanced Technology Research and Application Center, Ondokuz Mayis University, 55200, Atakum, Samsun, Turkiye
[2] Faculty of Art and Science, Kastamonu University, Department of Chemistry, 37150, Kastamonu, Turkiye
[3] Faculty of Education, Ondokuz Mayis University, Department of Chemistry Education, 55200, Atakum, Samsun, Turkiye
[4] Central Research Laboratory, Bartin University, 74100, Bartin, Turkiye
[5] Department of Pathology and Medical Biology, University of Groningen, University Medical Center Groningen, 9713 GZ Groningen, Netherlands
[6] Department of Medical Microbiology, School of Medicine, Acibadem Mehmet, Ali Aydınlar University, 34752 Atasehir, Istanbul, Turkiye
* Correspondence: nturkoz@omu.edu.tr; Tel.: +90- 535-7928967

Abstract: Biodiesel has several drawbacks, such as being prone to oxidation, having reduced stability, and having limited storage time. Antioxidants compatible with biodiesel are being used to address its drawbacks. The use of antioxidants in biodiesel has a significant impact on the environment and economy, especially in promoting sustainable energy. The study used blends consisting of 20% biodiesel and 80% diesel fuel. Isatin-thiosemicarbazones were tested as additives in blends at a concentration of 3000 parts per million (ppm) using an oxifast device. Comparing them to the chemical antioxidant Trolox. FT-IR, DSC, and TGA were used to characterize these samples. DSC measured sample crystallization temperatures (Tc). Samples with antioxidants showed decreased values compared to the non-antioxidant diesel sample D100. Several DSC tests were conducted to determine the antioxidant strengths of various samples. The results showed that the FT-IR spectrum's antioxidant effect regions grow clearer with antioxidants. The extra antioxidant is effective. Biodiesel's oxidative stability improves with isatin-thiosemicarbazones at varying concentrations. The kinetics of thermal decomposition of isatin-thiosemicarbazones under non-isothermal conditions have been determined using the Kissinger, Ozawa, and Boswell techniques. The activation energies of compounds **1** and **2** were calculated 137–147 kJ mol^{-1} and 173–183 kJ mol^{-1}, respectively.

Keywords: thiosemicarbazones; biodiesel; oxidative stability; kinetic study; energy

1. Introduction

The prediction indicates that there will be an increase in the utilization of fossil fuels to meet the growing energy demands. In recent years, there has been a growing body of research dedicated to exploring alternative fuel sources as a response to the detrimental effects of fossil resource consumption on environmental contamination [1]. The utilization of biodiesel offers a wide range of advantages. The non-toxic nature of this specific characteristic provides both safety and cost-effectiveness, making it a significant advantage [2]. The production of biodiesel is a complex process that involves several chemical reactions. These reactions lead to the formation of free radicals, which are highly reactive molecules that can easily undergo oxidation when exposed to the surrounding atmosphere [3]. In a study conducted, it was shown that the oxidation process has

 doi:10.20944/preprints202406.0056.v1

a negative impact on both fuel efficiency and engine performance [4]. The storage stability of biodiesel is crucial in assessing its overall quality. The significance of standards and fuel quality cannot be overstated [5].

Antioxidants are a group of molecules that effectively halt the process of oxidation. In order to effectively manage the oxidation of biodiesel, one method employed is the inhibition of free radical formation or the scavenging of existing radicals [6]. Antioxidants are commonly composed of phenolic functional groups within their chemical structure [7]. In recent studies, it has been discovered that the addition of both natural and synthetic antioxidants to biodiesel is crucial for improving and maximizing its oxidative stability. The significance of reducing the amount of free radicals in biodiesel and delaying oxidation is highlighted by the use of antioxidants [8]. The auto-oxidation mechanism involves the interruption of the peroxide radical (ROO·) progression by the antioxidant (AH), which inhibits the creation of an additional radical. The oxidation stability of biodiesel can be improved by incorporating antioxidants in specific proportions This addition serves to prevent the occurrence of oxidative reactions with antioxidant radicals [9]. The addition of antioxidants to biodiesel has been found to significantly improve its overall quality, extend its storage time, and enhance its durability [10].

The study of heterocyclic Schiff bases and their metallic complexes is of significant interest in the fields of chemistry, biology, and pharmacology [11, 12]. These compounds are formed through the primary amino groups of ketones or the condensation reaction of aldehydes [11, 13]. They exhibit various biological functions, including antioxidant [14], antifungal [14], antitumor [15], anticancer [16], antiviral [17], antimicrobial [18], and antimalarial properties [19]. Phenolic Schiff bases (SB-OH) exhibit antioxidant activity that is directly linked to their capacity to release hydrogen atoms [20]. Thiosemicarbazones are a notable category of synthetic chemicals that exhibit a diverse range of pharmacological and biological activities [21]. A diverse range of actions have been disclosed, including anti-HIV [22], anticancer [23], antimalarial [24], anticonvulsant [25], anti-inflammatory [26], antioxidant [27], anti-viral [28], enzymatic inhibition [29], antifungal [30], and antibacterial [31] properties. Isatin derivatives have demonstrated a wide range of biological activities, including antioxidant [32], antiviral [33], antifungal [34], antibacterial [35], antimicrobial [36], anti-HIV [22], antitubercular [37], and anticonvulsant [38] properties.

In this study, two previously synthesized isatin-thiosemicarbazones were used, whose chemical structures were elucidated by spectroscopic methods. Isatin-thiosemicarbazone derivatives were used to neutralize radical reactions in biodiesel-diesel fuel mixtures. Using a comparative analysis with Trolox, the antioxidant capacity of the compounds employed was confirmed. Trolox facilitates high-throughput screening for putative antioxidant capacity. These approaches are employed to evaluate the antioxidant capacity of biological samples such as plasma, individual chemicals, dietary components, or food extracts [40,41]. But it is believed that this synthetic antioxidant variant possesses hazardous and carcinogenic properties. Isatin-thiosemicarbazone derivatives were added, and a concentration of 3000 parts per million (ppm) was added to the mixtures. Several characterization techniques, including thermogravimetric analysis (TGA), differential scanning calorimetry (DSC), fourier-transform infrared spectroscopy (FT-IR), and the 1,1-diphenyl-2-picryl hydrazyl (DPPH·) assay, were used to evaluate the antioxidant activity of isatin-thiosemicarbazone derivatives. Also, the investigation of the breakdown kinetics of isatin-thiosemicarbazone derivatives was conducted using TGA. Non-isothermal experiments are more appropriate than isothermal kinetic studies for avoiding a rapid increase in temperature in the sample at the start. Conventional techniques that include fitting experimental data to the reaction model are not effective in providing accurate kinetic information for non-isothermal research. This is because these approaches fail to properly differentiate between the reaction model, f(α), and the temperature dependency, k(T). To address this drawback of model fitting, one might employ model-free isoconversional approaches. These approaches enable the determination of the activation energy based on conversion or temperature without making any assumptions about the reaction model [41].

Preprints.org (www.preprints.org) | NOT PEER-REVIEWED | Posted: 3 June 2024 doi:10.20944/preprints202406.0056.v1

2. Materials and Methods

2.1. Materials

Compounds from recognized suppliers such as Merck, Sigma, or Aldrich Chemical Company were used without further purification in their as-received form. Diesel fuel (D100) was given to OPET in Samsun, Turkey, while biodiesel (B100), made totally of waste sunflower and corn oil, was given to Aves Energy Oil and Food Industry in Mersin, Turkiye.

2.2. Methods

2.2.1. Schiff Based Isatin-Thiosemicarbazones Synthesis

Isatin-thiosemicarbazones were synthesized by reacting 5-methoxyisatin with thiosemicarbazides in aqueous ethanol and one drop of hydrochloric acid at reflux for three hours (Figure 1). The synthesis and characterization of the compounds have been performed previously by Muglu [42]. Physical data, melting points, and yields of the compounds are summarized in Table 1.

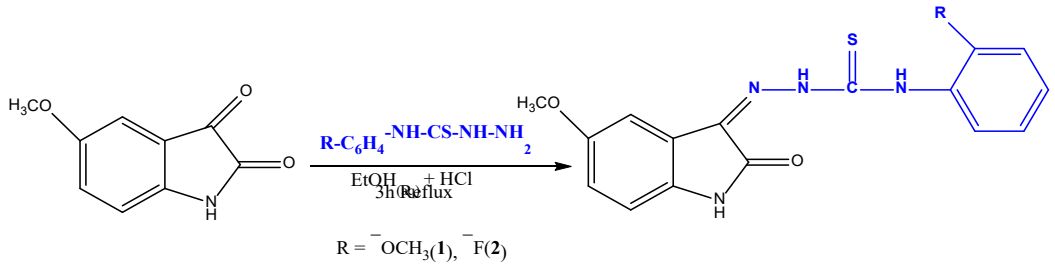

Figure 1. Synthetic route for Schiff-based isatin-thiosemicarbazones (**1-2**).

Table 1. Physical data of the synthesized compounds (**1-2**).

Compound code	R	Molecular formula	Molecular weight	Melting point (°C)	Yield %
1	2-OCH_3	$C_{17}H_{16}N_4O_3S$	356.41	218–220	87
2	2-F	$C_{16}H_{13}FN_4O_2S$	344.37	234–235	82

2.2.2. Preparations of Biodiesel-Diesel Blends

The ratio of biodiesel to diesel in diesel and biodiesel blends typically ranges from 20% to 80%. The mixture being blended is represented by the formula B20D80 [43]. In a recent study, researchers explored the potential benefits of combining extracts from various plants. The extracts were carefully blended together at a concentration of 3000 ppm. This concentration was chosen to ensure optimal effectiveness and maximize the potential benefits of the combined extracts. The researchers aimed to investigate the potential synergistic effects that could arise from this combination, as each plant extract may possess unique bioactive compounds. By combining these extracts, the researchers hoped to create a powerful formulation that could offer enhanced therapeutic properties [44]. Further research is needed to fully understand the implications and potential applications of Table 2. Various sample codes and content were presented.

Table 2. Exploring the contents and codes of blends containing biodiesel, diesel, antioxidants, and isatin-thiosemicarbazones.

Sample	Biodiesel (%)	Diesel (%)

 doi:10.20944/preprints202406.0056.v1

D100	-	100
B20D80	20	80
B20D80TROLOX	20	80
B20D80_2	20	80
B20D80_1	20	80

2.2.3. Differential Scanning Calorimetry (DSC)

DSC approaches can be utilized for the purposes of characterizing, quantifying, and inferring. The primary objective of this study was to investigate the temperatures at which crystallization begins (measured in degrees Celsius) for the materials D100, B30D70, B30D70BHT, B30D70_**2**, and B30D70_**1**. The experiment was carried out with a TA Q-2000 type calorimeter equipped with an RCS90 and a cooling system. Aluminum pans were utilized for the purpose of conducting analysis. In the course of this experimental process, a sample with a weight of 5 ± 0.5 mg was carefully positioned within the pan. The cooling rate throughout the temperature range of 25°C to -90°C was determined to be 10°C per minute, while a nitrogen flow rate of 50 mL per minute was maintained [45].

2.2.4. Thermogravimetric Analysis (TGA)

TGA is commonly employed to investigate the correlation between changes in mass and temperature variations, either rising or constant, within controlled air circumstances. This analytical methodology is utilized to quantify vapors, analyze combustion reactions, examine degradation processes, and ascertain residual components in products. The TGA technique has been employed to observe the decomposition characteristics of various organic compounds and the potential improvement of their constituents. TGA was performed using a SDT Q-600 instrument manufactured by TA Instrument-Waters, located in the United States. The collection of samples was achieved by subjecting five powder samples, each weighing 5 ± 0.5 mg, to a heating process at a rate of 10 °C per minute. This heating process took place in an alumina pan, and an oxygen gas flow of 50 mL per minute was maintained during the process. The temperature was increased until it reached 400 °C, as documented in reference. Thermal studies of isatin-thiosemicarbazone compounds were conducted using a Hitachi STA 7300. TGA, DTG, and DTA curves were obtained by measuring the thermal behavior of 3 mg samples at a heating rate of 10 °K min^{-1}. The experiment was conducted within a temperature range of 25–900 °C in a nitrogen environment with a flow rate of 100 mL min^{-1}. A crucible made of Al_2O_3 is utilized for conducting measurements [46].

2.2.5. Fourier Transform Infrared Spectroscopy (FT- IR)

FT-IR (Perkin Elmer, Spectrum-Two, USA) was used to analyze the chemical functional groups in isatin-thiosemicarbazone derivatives. The spectral region ranging from 650 to 4000 cm^{-1} was utilized for the purpose of scanning the surface of the sample. The ATR FT-IR spectra were obtained using an isothermal method at room temperature. At the beginning of our work, the background removal techniques, baseline correction, and data tune-up correction were implemented according to the procedure [47].

2.2.6. DPPH· Method for Antioxidant Activity

The DPPH· radical scavenging activity test was used to find out how effective the produced chemicals were as antioxidants. The free radical scavenging ability was assessed using the method of Brand-Williams et al. [48], with minor modifications. To assess antioxidant activity, the compounds were prepared in DMSO at a concentration of 250 µM. The compounds were dissolved in DMSO and then diluted to five different concentrations. The concentration of DPPH in ethanol was 50 µM. Different concentrations of compound solutions (5 µM, 10 µM, 20 µM, 50 µM, and 100 µM) were added to a previously prepared 5 mL DPPH solution, along with enough ethanol to

 doi:10.20944/preprints202406.0056.v1

make a total volume of 6 mL. The mixture was measured at 517 nm against a blank after being left for 30 minutes at room temperature in a dark room [49].

2.2.7. Kinetics of Isatin-Thiosemicarbazone Derivatives

The degradation of solids may be analyzed using a non-isothermal kinetic approach known as the model-free method. This method involves examining the temperature values associated with the reaction rate (α) in thermal analysis graphs obtained at various heating rates. Activation energies can also be calculated using this approach [50]. The thermal decomposition of isatin-thiosemicarbazone derivatives is a process that occurs in the solid state. The kinetics of this reaction may be broadly characterized by:

$$\frac{d(a)}{d(t)} = k(T).f(a) \quad (1)$$

The variables in the equation are as follows: t represents the reaction time in minutes, T represents the temperature in Kelvin, α represents the degree of conversion or reaction rate, k(T) represents the rate constant that depends on temperature, and f(α) represents the unique reaction model. The expression for k(T) can be represented using the Arrhenius equation:

$$k(T) = A.\exp\left(\frac{-E}{RT}\right) \quad (2)$$

Where A represents the exponential factor with units of min^{-1}, R represents the gas constant with units of 8.314 J mol^{-1} $°K^{-1}$, and E represents the activation energy with units of J mol^{-1}. The kinetic triples, consisting of the E, A, and f(α) values, are used to forecast the conversion degree of a chemical given the temperature [51].

$$ln\left(\frac{\beta}{T^2}\right) = ln\left[\frac{E.A}{R.g(a)}\right] - \left(\frac{E}{R.T}\right) \quad (3)$$

$$g(a) = \int_0^a f(a)^{-1}\, da \quad (4)$$

The activation energies for various α values may be determined by calculating the slope of the graph ln (β/T_2) – (1000/T) [52], using Equations (3) and (4).

$$\ln\left(\frac{\beta}{T^2}\right) = k_1 - \left(\frac{E}{R.T}\right) \quad (5)$$

$$\ln\left(\frac{\beta}{T}\right) = k_2 - \left(\frac{E}{R.T}\right) \quad (6)$$

$$\ln\,\beta = k_3 - 1{,}051\,\frac{E}{R.T} \quad (7)$$

Where k_1, k_2, and k_3 are fixed values. The activation energy was determined from the thermogravimetric curves using the Kissenger (Equation 5), Boswell (Equation 6), and Ozawa (Equation 7) techniques [41]. The thermogravimetric analysis tests were conducted using a Hitachi STA 7300 instrument at various heating rates (β = 5, 10, 15, 20 °K min^{-1}) in a N_2 environment with a flow rate of 100 mL min^{-1}. The temperature range for the studies was from ambient temperature to 1173 °K.

 doi:10.20944/preprints202406.0056.v1

3. Results and Discussion

3.1. Differential Scanning Calorimetry (DSC)

DSC measurements were conducted on a blend of fuel containing isatin-thiosemicarbazone derivatives and unbleached fuel in a nitrogen gas atmosphere. The resulting data is graphically shown in Figure 2.

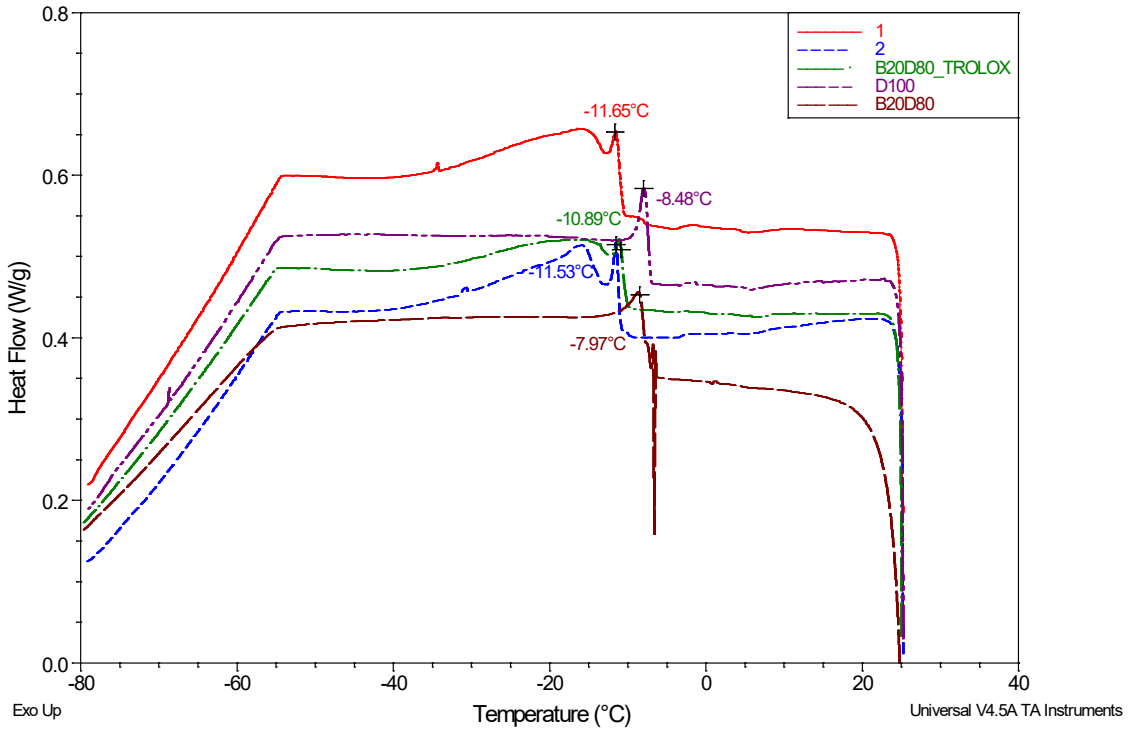

Figure 2. DSC thermograms of D100, B20D80, B20D80TROLOX, B20D80_**2**, and B20D80_**1** under N_2 atmosphere. The purpose of this research was to examine the effects of adding isatin-thiosemicarbazone derivatives to biodiesel-diesel blends on their crystallization temperatures. As a result, the study demonstrated that the extract derived from isatin-thiosemicarbazone derivatives had an increase in the crystallization point. This inquiry pertains to the initiation temperatures of crystallization for four distinct alloys, namely D100, B20D80, B20D80TROLOX, B20D80_**2**, and B20D80_**1**. After conducting experiments, the starting temperatures for crystallization were found to be -7.97 °C, -8.48 °C, -10.89 °C, -11.53 °C, and -11.65 °C for the samples marked D100, B20D80, B20D80TROLOX, B20D80_**2**, and B20D80_**1**, respectively, as seen in Table 3.

Table 3. Crystallization onset temperatures (°C) of D100, B20D80, B20D80TROLOX, B20D80_**2**, and B20D80_**1** determined using DSC in a N_2 atmosphere.

Sample	Crystallizations onset temperature (°C)
D100	7.97
B20D80	8.48
B20D80TROLOX	10.89
B20D80_2	11.53
B20D80_1	11.65

3.2. Thermogravimetric Analysis (TGA)

The compound of TGA-DTG graphs of several combinations were compared. It is observed that there is only one degree of degradation concerning temperature. The temperature at which degradation begins, known as the onset temperature, offers valuable information regarding thermal stability and the first boiling point. A positive association has been seen between the stability of the

 doi:10.20944/preprints202406.0056.v1

samples and the Tonset values, suggesting that an increase in sample stability is associated with a corresponding rise in Tonset values [53]. Figure 3 displays the graphical representations of the thermogravimetric analysis (TGA) and derivative thermogravimetric analysis (DrTGA) curves. Upon closer inspection, the curves are pretty like one another. At these temperatures, sample mass is lost between 98.56 and 99.36%. The values taken from the thermometers and recorded on the thermograms are listed in Table 4.

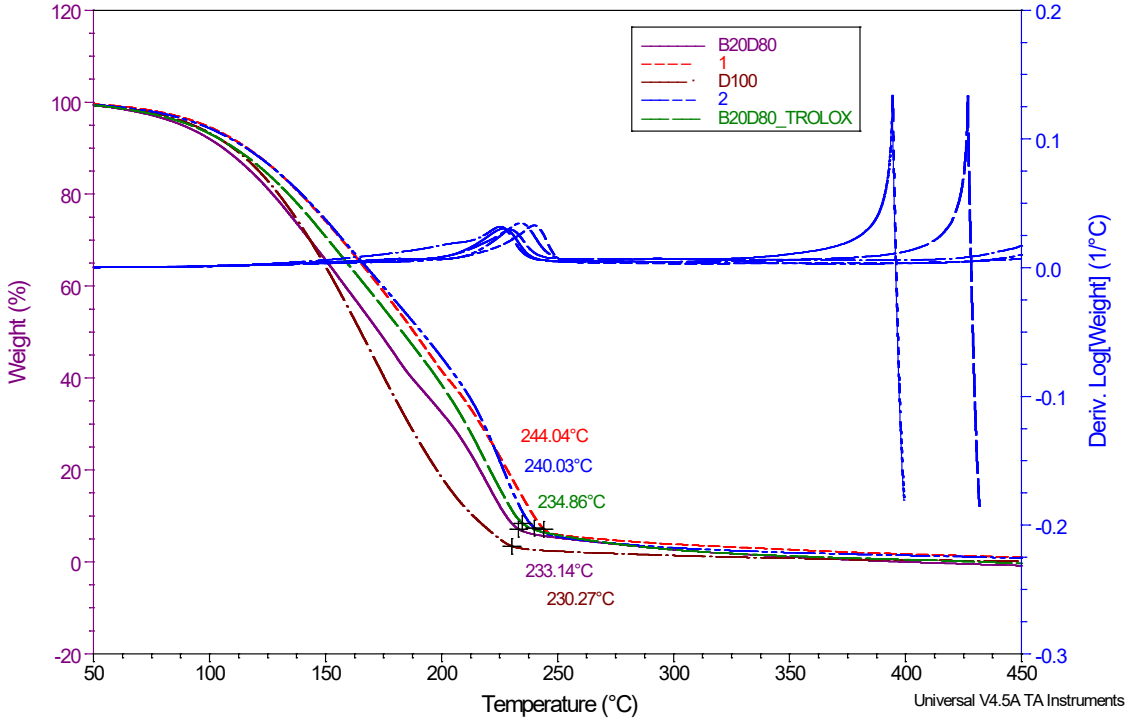

Figure 3. TGA and DrTGA curves of D100, B20D80, B20D80TROLOX, B20D80_**2**, and B20D80_**1** under O_2 atmosphere.

Table 4. Thermogravimetric analysis (TGA) of samples.

Sample name	Temperature range (°C)	Max, degradation temperature (°C) (Tonset)	Mass loss (%)
D100	25-250	99.36	11.52
B20D80	25-250	99.12	7.72
B20D80TROLOX	25-250	99.27	7.71
B20D80_2	25-250	99.24	8.94
B20D80_1	25-250	98.56	10.20

3.3. Fourier Transform Infrared Spectroscopy (FT- IR)

The FT-IR spectra of the biodiesel-diesel blends are depicted in Figure 4 (a–f). The impact of incorporating antioxidants at a concentration of 3000 ppm into biodiesel samples is displayed in Table 5. The valence-stretching vibration frequency range of an unbounded hydroxyl group, ν(O–H), is approximately 3661–3687 cm^{-1}. Spectral peaks in the range of 2925–3000 cm^{-1} are often associated with the vibration of ν(C–H) bonds, indicating oxidation. Aldehyde and ketone compounds in biodiesel samples contain these bonds, which are also found in antioxidants. The spectral range of 2925–2990 cm^{-1} is often linked to the ν(C–H) bending vibration, which is known to be involved in oxidation processes. Peaks in the 1079 cm^{-1} wavenumber indicate stretching of the ν(C-O) bond. The spectrum shows strong absorption bands, indicating the presence of the ester carbonyl functional group (C=O). The absorption is observed in the spectral range of 1746 cm^{-1}. The

 doi:10.20944/preprints202406.0056.v1

lack of a nearby band could suggest that carboxylic acids are not present. The bending vibrations of ν(N−H) are attributed to the observed vibrational modes at 1458 cm^{-1}. In isatin-thiocarbohydrazones, the bending vibrations of ν(C−N) occur within the range of 1199–1173 cm^{-1}. The long-term stability of biodiesel samples is linked to low oxidation levels [54]. Antioxidants, particularly phenolic chemicals, have been found to enhance peak intensity, according to studies.

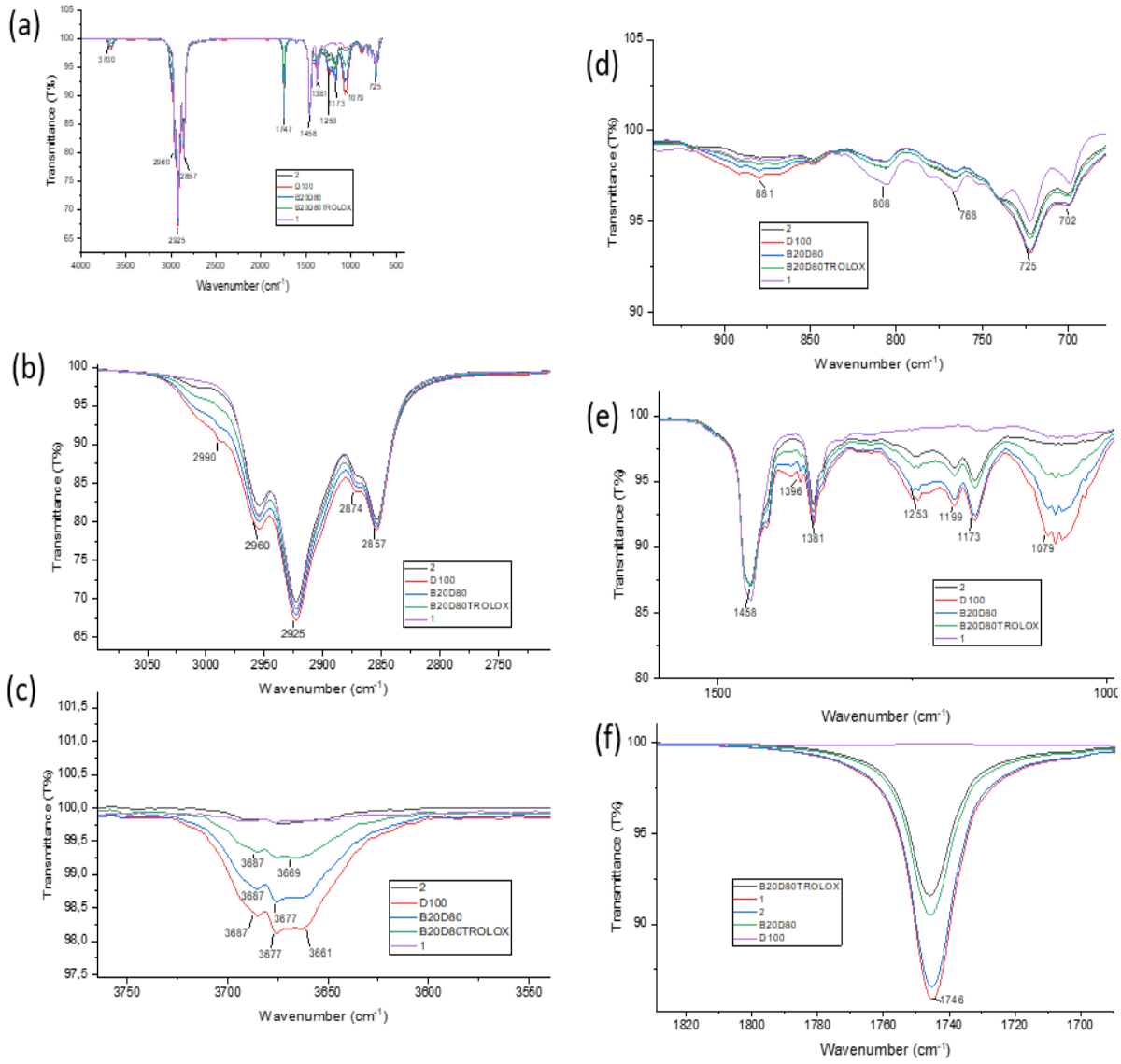

Figure 4. (**a**) FT-IR spectra of D100, B20D80, B20D80TROLOX, B20D80_**2**, and B20D80_**1** at 4000-500 cm^{-1}. (**b**) Antioxidant effects of D100, B20D80, B20D80TROLOX, B20D80_**2**, and B20D80_**1** samples between wavenumbers 2750 and 3050 cm^{-1}. **(c)** Antioxidant effects of D100, B20D80, B20D80TROLOX, B20D80_**2**, and B20D80_**1** samples between wavenumbers 3550 and 3750 cm^{-1}**.** (**d**) Antioxidant effects of D100, B20D80, B20D80TROLOX, B20D80_**2**, and B20D80_**1** samples between wavenumbers 700 and 900 cm^{-1}. **(e)** Antioxidant effects of D100, B20D80, B20D80TROLOX, B20D80_**2**, and B20D80_**1** samples between wavenumbers 1000 and 1500 cm^{-1}. (**f**) Antioxidant effects of D100, B20D80, B20D80TROLOX, B20D80_**2**, and B20D80_**1** samples between wavenumbers 1700 and 1820 cm^{-1}.

Table 5. Experimental FT-IR values of the compounds (cm^{-1}).

Compound	ν(O–H)	ν(C–H) Aromatic	ν(C–H) Aliphatic	ν(C=O)	ν(N–H)	ν(C–N)	ν(C–O)
B20D80_2	–	2925	2874	1746	1458	1199	1079

 doi:10.20944/preprints202406.0056.v1

B20D80_1	–	2925	2874	1746	1458	1173	1079
B20D80 TROLOX	3687	2925	2857	1746	–	–	1079
B20D80	3687	2925	2857	1746	–	–	1079
D100	3687	2925	2857	1746	–	–	1079

3.4. DPPH· Free Radical Scavenger Effect for Isatin-Thiosemicarbazones

The study assessed the samples' capacity to eliminate free radicals. Compound **1** had more activity with a value of 66.178 ± 0.11 µg/mL, whereas compound **2** showed lesser activity with a value of 79.927 ± 0.13 µg/mL. The arrangement of substituents in isatin-thiocarbohydrazones plays a vital role in determining their antioxidant activity, which is comparable to that of carbohydrazones [53]. The antioxidant activity of isatin-thiosemicarbazone derivatives can be attributed to the presence of substituted groups/atoms attached to the aromatic ring.

3.5. Thermal Characterization of Isatin-Thiosemicarbazones

Compound **1** is represented by the TGA, DTG, and DTA curves in Figure 5. The thermogravimetric (TGA) curve revealed that the thermal decomposition of compound **1** commenced at a temperature of 201 °C and exhibited two distinct stages of weight loss. The first and subsequent stages of weight loss account for 33.3% and 23.3%, respectively. The weight loss experienced from room temperature to 900 °C is precisely 69.8%. The differential thermogravimetric (DTG) curve of compound **1** exhibited two distinct peaks that corresponded to the thermogravimetric (TGA) curve. The initial stage was characterized by an exothermic peak at 213.3 °C observed in the DTA graph, indicating the melting point of the sample. The second stage was detected at a temperature of 265 °C on the DTA graph, and it manifested as an exothermic peak, indicating the thermal decomposition of compound **1**.

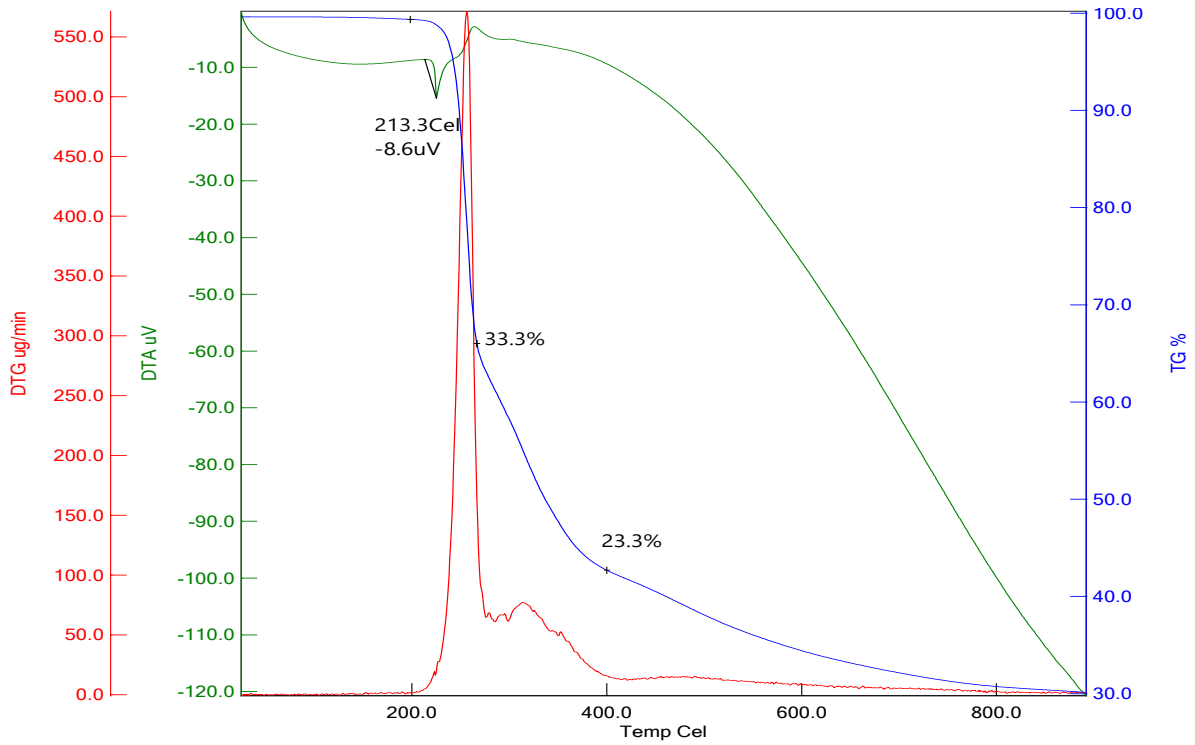

Figure 5. Studying the thermal properties of compound **1.**

Figure 6 displays the TGA, DTG, and DTA curves for compound **2**. The thermogravimetric (TGA) curve indicates that the decomposition begins around 218 °C and follows a two-step process. The initial stage of weight reduction accounts for 37.3%, whereas the subsequent stage accounts for 18.5%. The weight loss experienced from a temperature of 25 °C to 900 °C amounts to 69.9%. The

 doi:10.20944/preprints202406.0056.v1

DTG curve of compound **2** exhibited two peaks that corresponded to the TGA curve. The initial stage is associated with the determination of the melting point, as evidenced by the presence of an endothermic peak at 243.3 °C recorded on the DTA curve. The second stage is linked to thermal deterioration, as evidenced by the exothermic peak at 267 °C observed on the DTA curve [54].

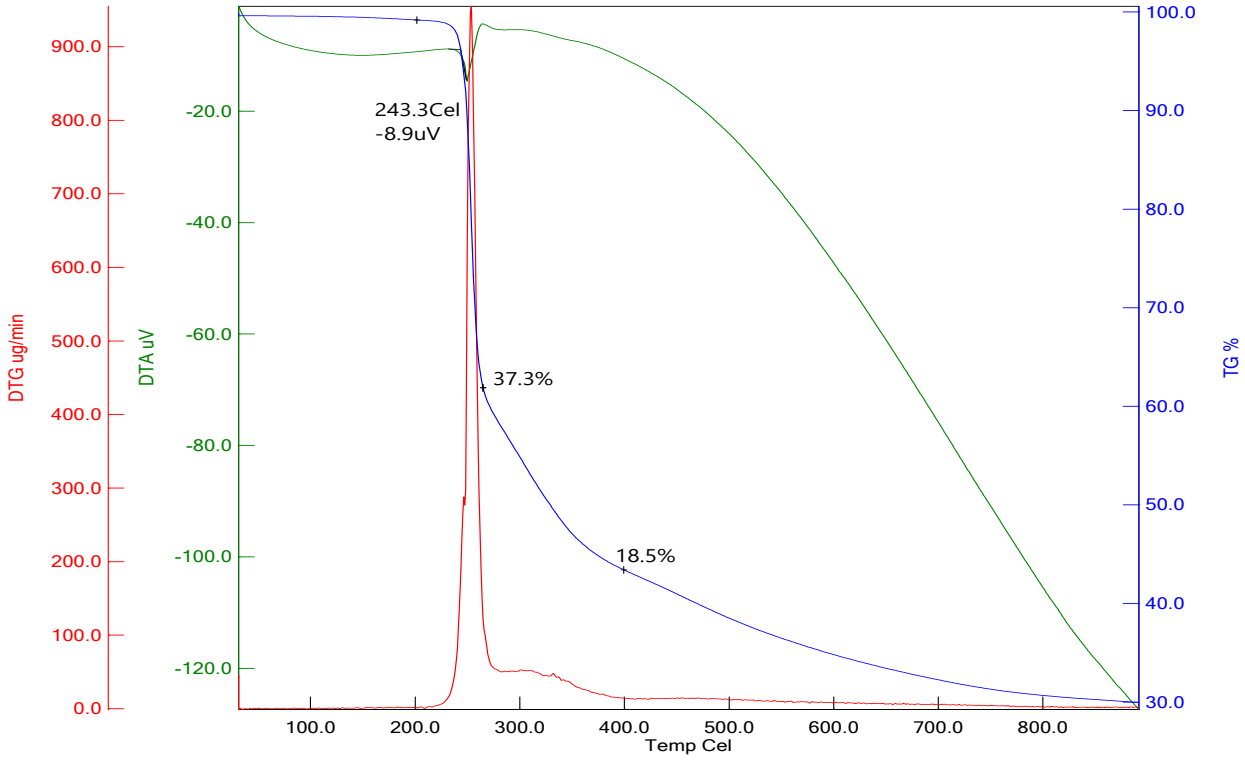

Figure 6. Studying the thermal properties of compound **2**.

3.6. Investigating the Kinetics of Isatin-Thiosemicarbazones

The TGA curves of compound **1** are displayed in Figure 7, depicting four continuous heating rates: 5, 10, 15, and 20 °C min^{-1}. As the heating rate increases from 5 to 20 °C, the TGA curves exhibit a rightward shift. Additionally, the peak temperature also changes towards a higher value with an increasing heating rate. Substantial reductions in weight were seen across all measures within the temperature range of 200–400 °C. Thermal decomposition occurs within the temperature range of 200 to 400 °C. Given that this phase has also been detected in the sample and its decomposition happens within the temperature range under investigation, it unavoidably impacts the kinetic curves [51].

 doi:10.20944/preprints202406.0056.v1

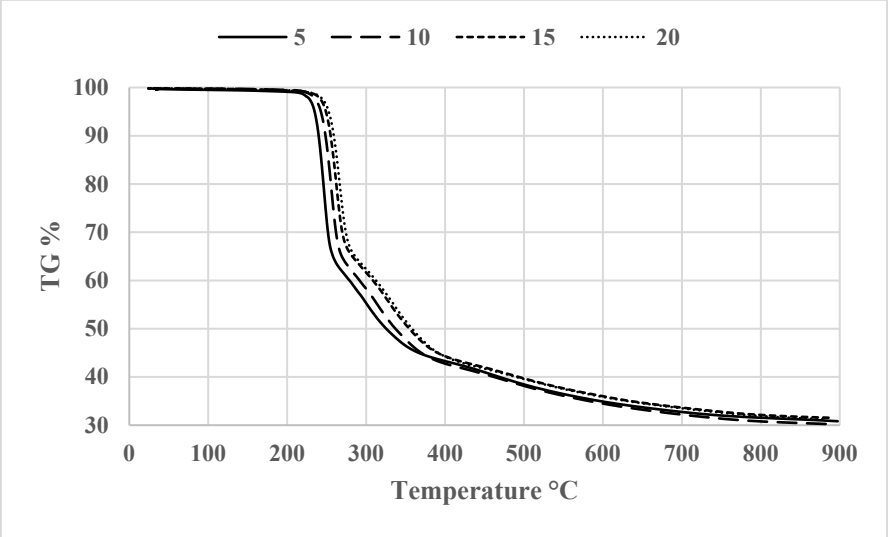

Figure 7. TGA curves of compound **1** at different heating rates.

Figure 8a depicts the temperature-response rate relationship for compound **1**, as represented by the curves. Figures 8b, 8c, and 8d display the diagrams used to calculate active tion energy using the Kissinger, Ozawa, and Boswell approaches, respectively. The activation energies obtained from the three approaches exhibit a high degree of similarity, as seen in Table 6. The activation energy values for the thermal decomposition process were determined using three different methods: the Kissinger approach yielded a value of 137.60 kJ mol^{-1}, the Ozawa method yielded a value of 146.58 kJ mol^{-1}, and the Boswell technique yielded a value of 142.09 kJ mol^{-1}. These calculations were performed under non-isothermal circumstances. Based on these results, it can be concluded that the activation energy needed for the decomposition of compound **1** falls within the range of 137–147 kJ mol^{-1}.

Preprints.org (www.preprints.org) | NOT PEER-REVIEWED | Posted: 3 June 2024 doi:10.20944/preprints202406.0056.v1

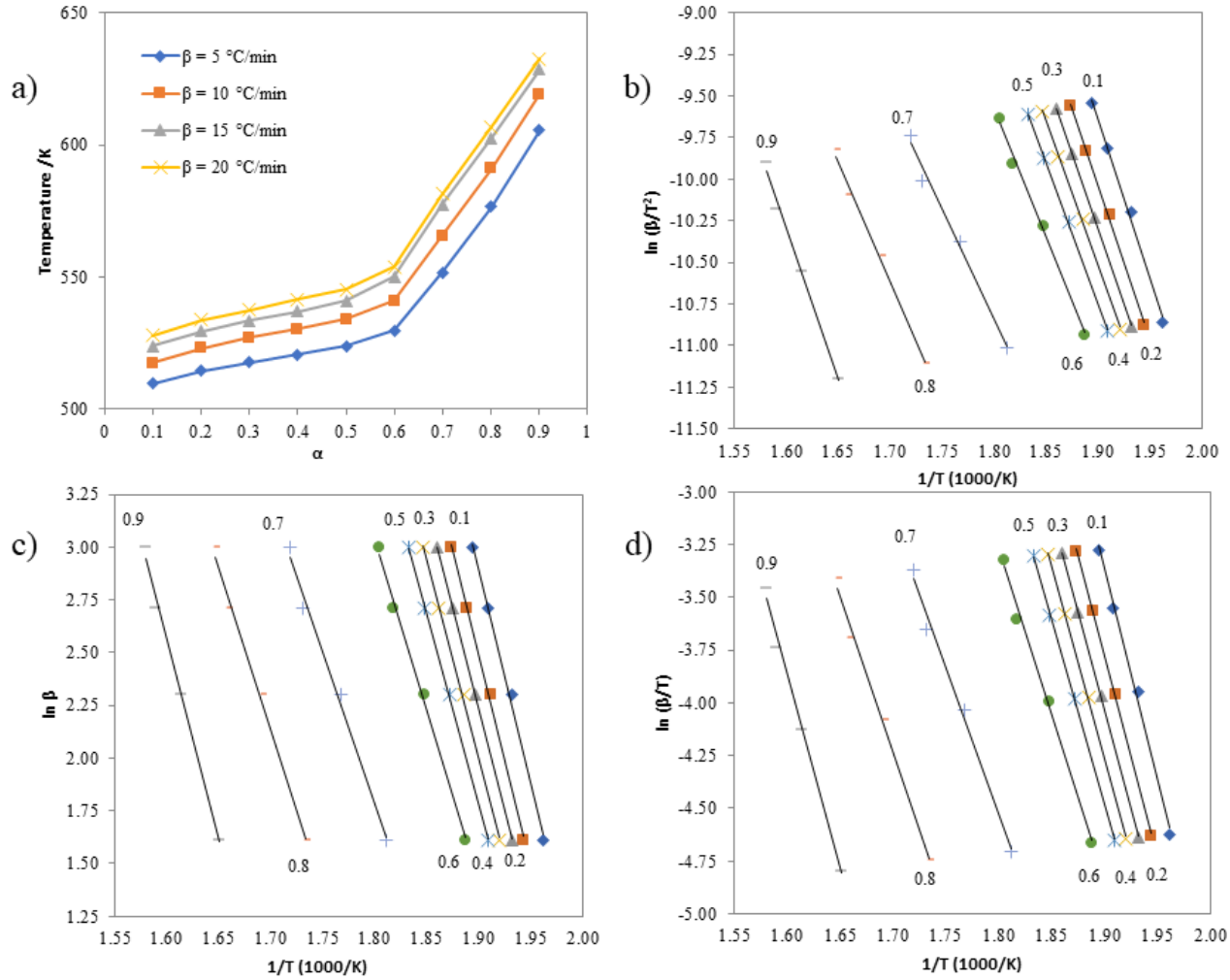

Figure 8. (**a**) Relationship between α and thermal decomposition temperature of the compound **1** at different heating rates, and Arrhenius plots for (**b**) Kissinger (**c**) Ozawa (**d**) Boswell methods.

Table 6. Calculating the relationship between activation energy values and -α using three methods for compound **1**.

α	Activation Energies (kJ mol-1)		
	Kissinger	Ozawa	Boswell
0.1	163.05	171.68	167.37
0.2	155.18	163.89	159.53
0.3	152.00	160.77	156.38
0.4	146.72	155.54	151.13
0.5	143.70	152.59	148.15
0.6	130.64	139.65	135.14
0.7	114.96	124.38	119.67
0.8	123.40	133.24	128.32
0.9	153.22	163.51	158.36

Figure 9 displays the thermogravimetric (TGA) curves of compound **2** obtained under several heating rates. Figure 9 demonstrates that the TGA curves changed towards higher temperatures as the heating rates increased. The temperature-α curves for compound **2** are shown in Figure 10a. The graphs illustrating the calculation of activation energy using the Kissinger, Ozawa, and Boswell

 doi:10.20944/preprints202406.0056.v1

approaches are displayed in Figures 10b, 10c, and 10d, respectively. The activation energy was calculated using the identical approaches for all three methods, and the corresponding findings are presented in Table 7. The activation energies for the thermal decomposition of compound **2**, as determined by the Kissinger, Ozawa, and Boswell techniques, were 173.61, 182.48, and 178.04 kJ mol^{-1}, respectively. Based on these figures, the amount of energy needed to decomposition compound **2** is between 173 and 183 kJ mol^{-1}.

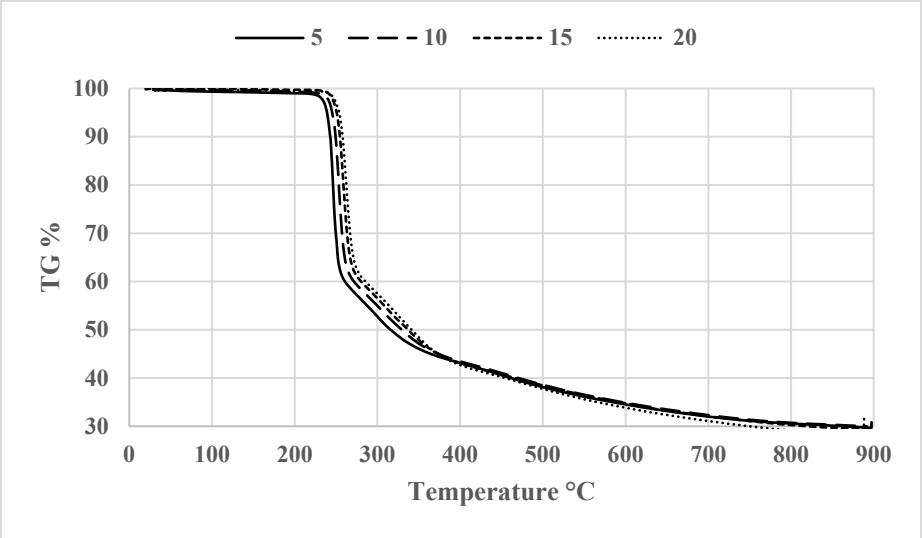

Figure 9. TGA curves of compound **2** at different heating rates.

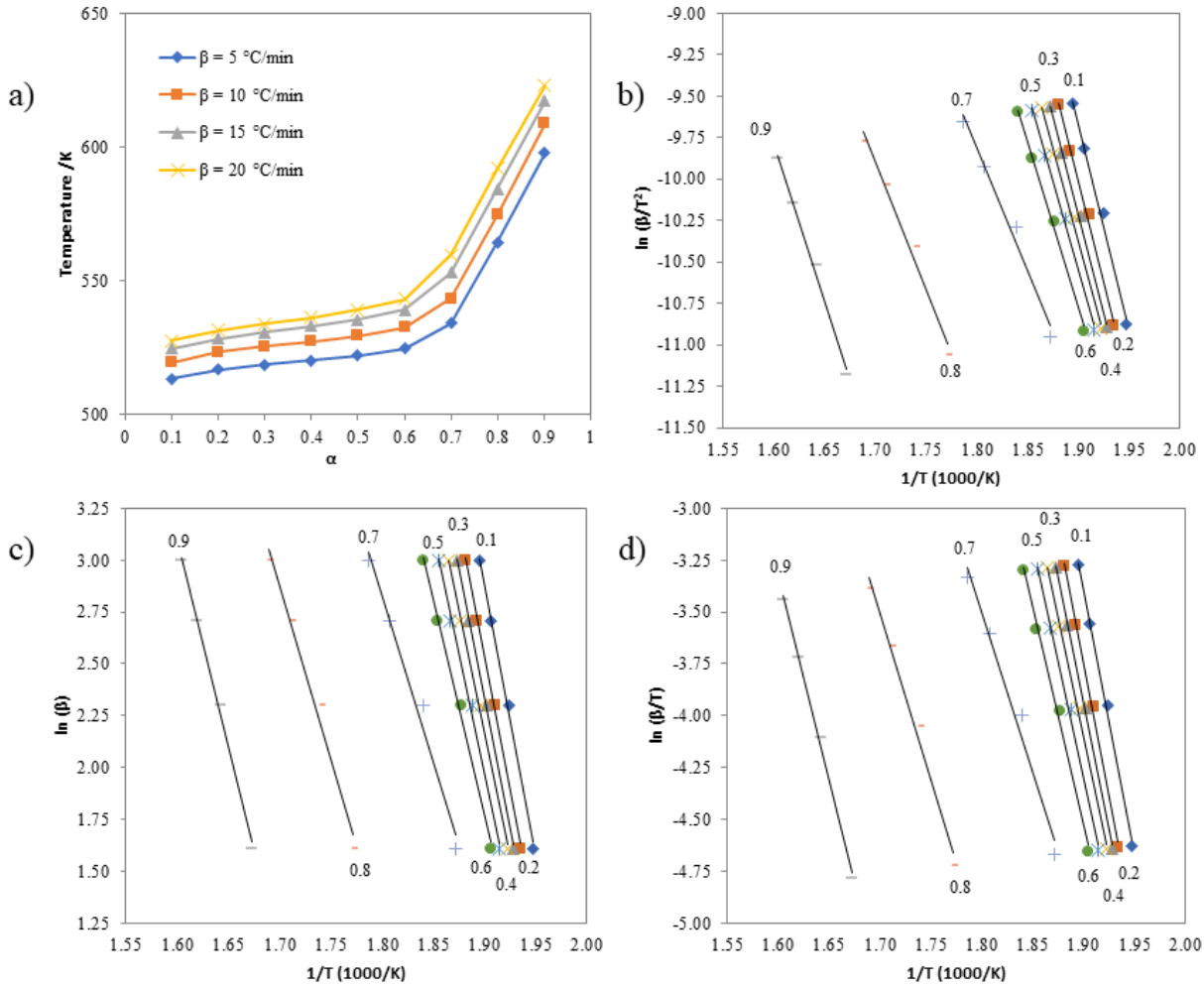

 doi:10.20944/preprints202406.0056.v1

Figure 10. (**a**) Relationship between α and thermal decomposition temperature of the compound **2** at various heating rates, and Arrhenius plots for (b**)** Kissinger (**c**) Ozawa (**d**) Boswell methods.

Table 7. Calculating the relationship between activation energy values and -α using three methods for compound **2**.

α	Activation Energies (kJ mol^{-1})		
	Kissinger	**Ozawa**	**Boswell**
0.1	211.74	220.40	216.07
0.2	206.48	215.19	210.83
0.3	199.63	208.38	204.01
0.4	190.60	199.38	194.99
0.5	182.53	191.35	186.94
0.6	169.41	178.29	173.85
0.7	125.89	134.98	130.44
0.8	129.56	139.17	134.36
0.9	160.42	170.57	165.49

The non-isothermal kinetic investigations of isatin-thiosemicarbazone derivatives revealed that the activation energy needed for the thermal decomposition of compound 1 is lower than that of compound 2. The thermal stability of compounds is directly proportional to their activation energy; a more extensive activation energy value indicates more excellent thermal stability [57]. Based on the findings of non-isothermal decomposition kinetics, compound 2 exhibits more incredible activation energy than compound 1. Compound 2 has superior heat stability. Additionally, it is recognized that the molecule with a lower activation energy exhibits superior antioxidant capabilities [58]. Therefore, it has been verified that compound 1, which shows a greater yield, possesses superior antioxidant characteristics.

5. Conclusions

Biodiesel is an environmentally friendly and cost-effective alternative to traditional diesel fuel. Our research focused on addressing the instability of biodiesel caused by its high susceptibility to oxidation. The outcomes of our study are summarized below:

The DSC results are as follows: Using natural and synthetic antioxidants can significantly raise the crystallization temperature (Tc). The crystallization temperatures of multiple samples ranged from -11.76 °C to -13.97 °C. Lower temperatures were found to be a sign of increased purity in the samples being studied. The start of crystallization was determined by measuring the temperatures at which it began. A study was conducted to analyze different samples and record their temperatures. Two samples, D100 and B30D70, were tested for temperature. D100 had a temperature of -11.76 °C, while B30D70 had a slightly lower temperature of -11.87 °C. The B30D70TROLOX sample had a temperature of -12.03 °C, while B30D70_**2** had a slightly lower temperature of -12.73 °C. The sample B30D70_**1** had the lowest temperature of -13.97 °C among all the samples. The findings shed light on the temperature characteristics of the analyzed samples in this study. B30D70, B30D70TROLOX, B30D70_**2**, and B30D70_**1** have lower crystallization tendencies than D100 in the realm of crystallization. The incorporation of antioxidants enhances oxidation stability. The substance mentioned has early crystallization, rapid oxidation, and is highly susceptible to oxidation. The stability of the characteristic increases sequentially. The addition of Schiff base_**1** increased the fuel blends' crystallization point by 87.78%, while Schiff base_**2** increased it by 72.16%.

The TGA results showed that the samples D100, B30D70, B30D70TROLOX, B30D70_**2**, and B30D70_**1** underwent oxidative degradation between 25 and 275 °C. The degradation process occurred in one step. In thermal dynamics, mass loss occurs within certain temperature ranges.

 doi:10.20944/preprints202406.0056.v1

Recent studies have found that this occurrence happens between 98.09% and 99.44% in the different samples studied. The curves show similarities with slight differences in Tonset values among the biodiesel-diesel samples.

FT-IR was used to identify functional groups in the samples. The presence of functional groups in biodiesel-diesel blends, specifically B30D70_**2** and B30D70_**1**, was found to be lower compared to other samples like B30D70TROLOX. This decrease can be attributed to the addition of 3000 ppm of Schiff bases. Incorporating Schiff bases into the composite has improved its oxidative stability, according to the mentioned discovery.

The compounds' antioxidant properties were tested using their DPPH· free radical activities. The tests used the spectrophotometric method and scavenging techniques. The synthesized isatin-thiosemicarbazones showed IC_{50} values of 66.178 ± 0.11 μg/mL and 79.927 ± 0.13 μg/mL for DPPH· free radical scavenging activity. Compound **1** exhibited the highest antioxidant activity among the evaluated compounds, but had less activity than standard Trolox. A study was conducted to examine the connection between the compound's structure and its activity. The investigation studied substituents and their characteristics. Isatin-thiosemicarbazones were synthesized and used as antioxidants to minimize the disadvantages of biodiesel, which is a more efficient alternative to fossil diesel fuel.

The study also focused on examining the activation energies associated with the thermal decomposition of isatin-thiosemicarbazone derivatives. This was accomplished by examining non-isothermal thermogravimetric (TGA) curves at different heating rates (5, 10, 15, 20 °K min^{-1}). The activation energy values for compounds **1** and **2** were determined using the Kissinger, Ozawa, and Boswell techniques, yielding values of 137–147 kJ mol^{-1} and 173–183 kJ mol^{-1}, respectively. As a result, it was discovered that the molecule with a lower activation energy exhibited superior antioxidant effects.

6. Patents

This section is not mandatory but may be added if there are patents resulting from the work reported in this manuscript.

Author Contributions: Nalan Turkoz Karakullukcu; Formal analysis, funding acquisition, validation, writing – review & editing, investigation, resources, supervision, project administration. **Halit Muglu;** Formal analysis, investigation, writing – original draft, resources, data curation. **Hasan Yakan;** Formal analysis, investigation, supervision, writing – original draft, data curation. **Volkan Murat Yilmaz;** Conceptualization, formal analysis, writing – original draft, investigation, software. **Ikbal Agah Ince;** Formal analysis, supervision, writing – review & editing, visualition, software.

Data Availability Statement: Data will be made available on request.

Funding: This research received no external funding.

Institutional Review Board Statement: Not applicable.

Informed Consent Statement: Not applicable.

Data Availability Statement: Data are contained within the article.

Conflicts of Interest: The authors declare no conflict of interest.

References

1. Atabani, A.E.; Silitonga, A.S.; Badruddin, I.A.; Mahlia, T.M.I.; Masjuki, H.H.; Mekhilef, S. A Comprehensive Review on Biodiesel as an Alternative Energy Resource and Its Characteristics. *Renewable and Sustainable Energy Reviews* **2012**, *16*, 2070–2093. https://doi.org/10.1016/j.rser.2012.01.003.
2. Srivastava, A.; Prasad, R. Triglycerides-Based Diesel Fuels. *Renewable & sustainable energy reviews* **2000**, *4*, 111–133. https://doi.org/10.1016/S1364-0321(99)00013-1.
3. Hosseinzadeh-bandbafha, H.; Kumar, D.; Singh, B.; Shahbeig, H. Biodiesel Antioxidants and Their Impact on the Behavior of Diesel Engines : A Comprehensive Review. *Fuel Processing Technology* **2022**, *232*, 107264. https://doi.org/10.1016/j.fuproc.2022.107264.

4. Ravi Krishna, E.; Muralidhar Reddy, P.; Sarangapani, M.; Hanmanthu, G.; Geeta, B.; Shoba Rani, K.; Ravinder, V. Synthesis of N4 Donor Macrocyclic Schiff Base Ligands and Their Ru (II), Pd (II), Pt (II) Metal Complexes for Biological Studies and Catalytic Oxidation of Didanosine in Pharmaceuticals. *Spectrochimica Acta - Part A: Molecular and Biomolecular Spectroscopy* **2012**, *97*, 189–196. https://doi.org/10.1016/j.saa.2012.05.073.
5. Kumar, R.; Kumar, V.; Sham, R. Stability of Biodiesel – A Review. *Renewable and Sustainable Energy Reviews* **2016**, *62*, 866–881. https://doi.org/10.1016/j.rser.2016.05.001.
6. Fang, H.L.; McCormick, R.L. Spectroscopic Study of Biodiesel Degradation Pathways. *SAE Technical Papers* **2006**, 776–790. https://doi.org/10.4271/2006-01-3300.
7. Abbas, M.; Saeed, F.; Anjum, F.M.; Afzaal, M.; Tufail, T.; Bashir, M.S.; Ishtiaq, A.; Hussain, S.; Suleria, H.A.R. Natural Polyphenols: An Overview. *International Journal of Food Properties* **2017**, *20*, 1689–1699. https://doi.org/10.1080/10942912.2016.1220393.
8. Rizwanul Fattah, I.M.; Masjuki, H.H.; Kalam, M.A.; Hazrat, M.A.; Masum, B.M.; Imtenan, S.; Ashraful, A.M. Effect of Antioxidants on Oxidation Stability of Biodiesel Derived from Vegetable and Animal Based Feedstocks. *Renewable and Sustainable Energy Reviews* **2014**, *30*, 356–370. https://doi.org/10.1016/j.rser.2013.10.026.
9. Pullen, J.; Saeed, K. An Overview of Biodiesel Oxidation Stability. *Renewable and Sustainable Energy Reviews* **2012**, *16*, 5924–5950. https://doi.org/10.1016/j.rser.2012.06.024.
10. Rashedul, H.K.; Masjuki, H.H.; Kalam, M.A.; Teoh, Y.H.; How, H.G.; Rizwanul Fattah, I.M. Effect of Antioxidant on the Oxidation Stability and Combustion-Performance-Emission Characteristics of a Diesel Engine Fueled with Diesel-Biodiesel Blend. *Energy Conversion and Management* **2015**, *106*, 849–858. https://doi.org/10.1016/j.enconman.2015.10.024.
11. Uddin, M.N.; Ahmed, S.S.; Alam, S.M.R. REVIEW: Biomedical Applications of Schiff Base Metal Complexes. *Journal of Coordination Chemistry* **2020**, *73*, 3109–3149. https://doi.org/10.1080/00958972.2020.1854745.
12. Koteswara Rao, N.S.R.R.M.M.; Ram Reddy, M.G. Studies on the Synthesis, Characterisation and Antimicrobial Activity of New Co(II), Ni(II) and Zn(II) Complexes of Schiff Base Derived from Ninhydrin and Glycine. *Biology of Metals* **1990**, *3*, 19–23. https://doi.org/10.1007/BF01141172.
13. Kalem, E.; Ağar, E. Schiff Bazlarinin Biyolojik Aktivitesi Biological Activity of Schiff Bases Öz : Abstract : **2021**, *8*, 57–76.
14. Chen, Y.; Mi, Y.; Li, Q.; Dong, F.; Guo, Z. Synthesis of Schiff Bases Modified Inulin Derivatives for Potential Antifungal and Antioxidant Applications. *International Journal of Biological Macromolecules* **2020**, *143*, 714–723. https://doi.org/10.1016/j.ijbiomac.2019.09.127.
15. Ren, S.; Wang, R.; Komatsu, K.; Bonaz-Krause, P.; Zyrianov, Y.; McKenna, C.E.; Csipke, C.; Tokes, Z.A.; Lien, E.J. Synthesis, Biological Evaluation, and Quantitative Structure -Activity Relationship Analysis of New Schiff Bases of Hydroxysemicarbazide as Potential Antitumor Agents. *Journal of Medicinal Chemistry* **2002**, *45*, 410–419. https://doi.org/10.1021/jm010252q.
16. Duff, B.; Reddy Thangella, V.; Creaven, B.S.; Walsh, M.; Egan, D.A. Anti-Cancer Activity and Mutagenic Potential of Novel Copper(II) Quinolinone Schiff Base Complexes in Hepatocarcinoma Cells. *European Journal of Pharmacology* **2012**, *689*, 45–55. https://doi.org/10.1016/j.ejphar.2012.06.004.
17. Jarrahpour, A.; Sheikh, J.; Mounsi, I. El; Juneja, H.; Hadda, T. Ben Computational Evaluation and Experimental in Vitro Antibacterial, Antifungal and Antiviral Activity of Bis-Schiff Bases of Isatin and Its Derivatives. *Medicinal Chemistry Research* **2013**, *22*, 1203–1211. https://doi.org/10.1007/s00044-012-0127-6.
18. Singh, K.; Raparia, S.; Surain, P. Co(II), Ni(II), Cu(II) and Zn(II) Complexes of 4-(4-Cyanobenzylideneamino)-3-Mercapto-5-Oxo-1,2,4-Triazine: Synthesis, Characterization and Biological Studies. *Medicinal Chemistry Research* **2015**, *24*, 2336–2346. https://doi.org/10.1007/s00044-014-1298-0.
19. Tople, M.S.; Patel, N.B.; Patel, P.P.; Purohit, A.C.; Ahmad, I.; Patel, H. An in Silico-in Vitro Antimalarial and Antimicrobial Investigation of Newer 7-Chloroquinoline Based Schiff-Bases. *Journal of Molecular Structure* **2023**, *1271*, 134016. https://doi.org/10.1016/j.molstruc.2022.134016.
20. Petrović, Z.D.; Orović, J.; Simijonović, D.; Petrović, V.P.; Marković, Z. Experimental and Theoretical Study of Antioxidative Properties of Some Salicylaldehyde and Vanillic Schiff Bases. *RSC Advances* **2015**, *5*, 24094–24100. https://doi.org/10.1039/c5ra02134k.
21. Bharti, S.K.; Nath, G.; Tilak, R.; Singh, S.K. Synthesis, Anti-Bacterial and Anti-Fungal Activities of Some Novel Schiff Bases Containing 2,4-Disubstituted Thiazole Ring. *European Journal of Medicinal Chemistry* **2010**, *45*, 651–660. https://doi.org/10.1016/j.ejmech.2009.11.008.
22. Bal, T.R.; Anand, B.; Yogeeswari, P.; Sriram, D. Synthesis and Evaluation of Anti-HIV Activity of Isatin β-Thiosemicarbazone Derivatives. *Bioorganic and Medicinal Chemistry Letters* **2005**, *15*, 4451–4455. https://doi.org/10.1016/j.bmcl.2005.07.046.
23. Cvijetić, I.N.; Herlah, B.; Marinković, A.; Perdih, A.; Bjelogrlić, S.K. Phenotypic Discovery of Thiocarbohydrazone with Anticancer Properties and Catalytic Inhibition of Human DNA Topoisomerase IIα. *Pharmaceuticals* **2023**, *16*, 341. https://doi.org/10.3390/ph16030341.

24. de Oliveira, R.B.; de Souza-Fagundes, E.M.; Soares, R.P.P.; Andrade, A.A.; Krettli, A.U.; Zani, C.L. Synthesis and Antimalarial Activity of Semicarbazone and Thiosemicarbazone Derivatives. *European Journal of Medicinal Chemistry* **2008**, *43*, 1983–1988. https://doi.org/10.1016/j.ejmech.2007.11.012.
25. Fayed, E.A.; Ragab, A.; Ezz Eldin, R.R.; Bayoumi, A.H.; Ammar, Y.A. In Vivo Screening and Toxicity Studies of Indolinone Incorporated Thiosemicarbazone, Thiazole and Piperidinosulfonyl Moieties as Anticonvulsant Agents. *Bioorganic Chemistry* **2021**, *116*, 105300. https://doi.org/10.1016/j.bioorg.2021.105300.
26. Jacob, Í.T.T.; Gomes, F.O.S.; de Miranda, M.D.S.; de Almeida, S.M.V.; da Cruz-Filho, I.J.; Peixoto, C.A.; da Silva, T.G.; Moreira, D.R.M.; de Melo, C.M.L.; de Oliveira, J.F.; et al. Anti-Inflammatory Activity of Novel Thiosemicarbazone Compounds Indole-Based as COX Inhibitors. *Pharmacological Reports* **2021**, *73*, 907–925. https://doi.org/10.1007/s43440-021-00221-7.
27. Yakan, H. Preparation, Structure Elucidation, and Antioxidant Activity of New Bis(Thiosemicarbazone) Derivatives. *Turkish Journal of Chemistry* **2020**, *44*, 1085–1099. https://doi.org/10.3906/KIM-2002-76.
28. Pelosi, G.; Bisceglie, F.; Bignami, F.; Ronzi, P.; Schiavone, P.; Re, M.C.; Casoli, C.; Pilotti, E. Antiretroviral Activity of Thiosemicarbazone Metal Complexes. *Journal of Medicinal Chemistry* **2010**, *53*, 8765–8769. https://doi.org/10.1021/jm1007616.
29. Yakan, H.; Muğlu, H.; Türkeş, C.; Demir, Y.; Erdoğan, M.; Çavuş, M.S.; Beydemir, Ş. A Novel Series of Thiosemicarbazone Hybrid Scaffolds: Design, Synthesis, DFT Studies, Metabolic Enzyme Inhibition Properties, and Molecular Docking Calculations. *Journal of Molecular Structure* **2023**, *1280*. https://doi.org/10.1016/j.molstruc.2023.135077.
30. Qin, Y.; Xing, R.; Liu, S.; Li, K.; Meng, X.; Li, R.; Cui, J.; Li, B.; Li, P. Novel Thiosemicarbazone Chitosan Derivatives: Preparation, Characterization, and Antifungal Activity. *Carbohydrate Polymers* **2012**, *87*, 2664–2670. https://doi.org/10.1016/j.carbpol.2011.11.048.
31. Khan, S.A.; Kumar, P.; Joshi, R.; Iqbal, P.F.; Saleem, K. Synthesis and in Vitro Antibacterial Activity of New Steroidal Thiosemicarbazone Derivatives. *European Journal of Medicinal Chemistry* **2008**, *43*, 2029–2034. https://doi.org/10.1016/j.ejmech.2007.12.004.
32. Andreani, A.; Burnelli, S.; Granaiola, M.; Leoni, A.; Locatelli, A.; Morigi, R.; Rambaldi, M.; Varoli, L.; Cremonini, M.A.; Placucci, G.; et al. New Isatin Derivatives with Antioxidant Activity. *European Journal of Medicinal Chemistry* **2010**, *45*, 1374–1378. https://doi.org/10.1016/j.ejmech.2009.12.035.
33. Elsaman, T.; Mohamed, M.S.; Eltayib, E.M.; Abdel-aziz, H.A.; Abdalla, A.E.; Munir, M.U.; Mohamed, M.A. Isatin Derivatives as Broad-Spectrum Antiviral Agents: The Current Landscape. *Medicinal Chemistry Research* **2022**, *31*, 244–273. https://doi.org/10.1007/s00044-021-02832-4.
34. Chohan, Z.H.; Pervez, H.; Rauf, A.; Khan, K.M.; Supuran, C.T. Isatin-Derived Antibacterial and Antifungal Compounds and Their Transition Metal Complexes. *Journal of Enzyme Inhibition and Medicinal Chemistry* **2004**, *19*, 417–423. https://doi.org/10.1080/14756360410001710383.
35. Guo, H. Isatin Derivatives and Their Anti-Bacterial Activities. *European Journal of Medicinal Chemistry* **2019**, *164*, 678–688. https://doi.org/10.1016/j.ejmech.2018.12.017.
36. Tangadanchu, V.K.R.; Sui, Y.F.; Zhou, C.H. Isatin-Derived Azoles as New Potential Antimicrobial Agents: Design, Synthesis and Biological Evaluation. *Bioorganic and Medicinal Chemistry Letters* **2021**, *41*, 128030. https://doi.org/10.1016/j.bmcl.2021.128030.
37. Jiang, D.; Wang, G.Q.; Liu, X.; Zhang, Z.; Feng, L.S.; Liu, M.L. Isatin Derivatives with Potential Antitubercular Activities. *Journal of Heterocyclic Chemistry* **2018**, *55*, 1263–1279. https://doi.org/10.1002/jhet.3189.
38. Nain, S. Recent Advancement in Synthesis of Isatin as Anticonvulsant Agents: A Review. *Medicinal Chemistry* **2014**, *4*. https://doi.org/10.4172/2161-0444.1000173.
39. Van Den Berg, R.; Haenen, G.R.M.M.; Van Den Berg, H.; Bast, A. Applicability of an Improved Trolox Equivalent Antioxidant Capacity (TEAC) Assay for Evaluation of Antioxidant Capacity Measurements of Mixtures. *Food Chemistry* **1999**, *66*, 511–517. https://doi.org/10.1016/S0308-8146(99)00089-8.
40. Lúcio, M.; Nunes, C.; Gaspar, D.; Ferreira, H.; Lima, J.L.F.C.; Reis, S. Antioxidant Activity of Vitamin E and Trolox: Understanding of the Factors That Govern Lipid Peroxidation Studies in Vitro. *Food Biophysics* **2009**, *4*, 312–320. https://doi.org/10.1007/s11483-009-9129-4.
41. Volkan, Y.M. Investigation of The Evaluation of Diasporic Bauxite from Islahiye Region in Alumina Production, Sakarya University, 2022.
42. Muğlu, H. Synthesis, Characterization, and Antioxidant Activity of Some New N 4-Arylsubstituted-5-Methoxyisatin-β-Thiosemicarbazone Derivatives. *Research on Chemical Intermediates* **2020**, *46*, 2083–2098. https://doi.org/10.1007/s11164-020-04079-x.
43. Wang, X.; Dai, M.; Xie, Y.; Han, J.; Ma, Y.; Chen, C. Experimental Investigation of Evaporation Characteristics of Biodiesel-Diesel Blend Droplets with Carbon Nanotubes and Nanoceria as Nanoadditives. *Applied Surface Science* **2020**, *505*, 144186. https://doi.org/10.1016/j.apsusc.2019.144186.
44. Dunn, R.O. Effect of Antioxidants on the Oxidative Stability of Methyl Soyate (Biodiesel) B. **2005**, *86*, 1071–1085. https://doi.org/10.1016/j.fuproc.2004.11.003.

45. Maru, M.M.; Lucchese, M.M.; Legnani, C.; Quirino, W.G.; Balbo, A.; Aranha, I.B.; Costa, L.T.; Vilani, C.; de Sena, L.Á.; Damasceno, J.C.; et al. Biodiesel Compatibility with Carbon Steel and HDPE Parts. *Fuel Processing Technology* **2009**, *90*, 1175–1182. https://doi.org/10.1016/j.fuproc.2009.05.014.
46. Aniza, R.; Chen, W.H.; Kwon, E.E.; Bach, Q.V.; Hoang, A.T. Lignocellulosic Biofuel Properties and Reactivity Analyzed by Thermogravimetric Analysis (TGA) toward Zero Carbon Scheme: A Critical Review. *Energy Conversion and Management: X* **2024**, *22*, 100538. https://doi.org/10.1016/j.ecmx.2024.100538.
47. Kutuk, H.; Turkoz, N. Microwave-Assisted Synthesis of Disulfides. *Phosphorus, Sulfur and Silicon and the Related Elements* **2011**, *186*, 1515–1522. https://doi.org/10.1080/10426507.2010.520174.
48. Brand-Williams, W.; Cuvelier, M.E.; Berset, C. Use of a Free Radical Method to Evaluate Antioxidant Activity. *LWT - Food Science and Technology* **1995**, *28*, 25–30. https://doi.org/10.1016/S0023-6438(95)80008-5.
49. Yakan, H.; Cakmak, S.; Kutuk, H.; Yenigun, S.; Ozen, T. Synthesis, Characterization, Antioxidant, and Antibacterial Activities of New 2,3-Dimethoxy and 3-Acetoxy-2-Methyl Benzamides. *Research on Chemical Intermediates* **2020**, *46*, 2767–2787. https://doi.org/10.1007/s11164-020-04118-7.
50. Haji, I., Yildız, K. Decomposition Kinetics of Diasporitic Bauxite from Gaziantep Region. In Proceedings of the 9th International Scientific Research Congress, Ankara.; 2021; pp. 439–447.
51. Angelopoulos, P, Samouhos, M, Taxiarchou, M. Thermal Decomposition Kinetics of Greek Diasporic Bauxite. *Proceedings of OPMR 2016- Opportunities in Processing of Metal Resources in South East Europe* **2016**, 191–200.
52. Küçük, F.; Yildiz, K. The Decomposition Kinetics of Mechanically Activated Alunite Ore in Air Atmosphere by Thermogravimetry. *Thermochimica Acta* **2006**, *448*, 107–110. https://doi.org/10.1016/j.tca.2006.07.003.
53. Çavuş, M.S.; Yakan, H.; Muğlu, H.; Bakır, T. Novel Carbohydrazones Including 5-Substituted Isatin: Synthesis, Characterization, and Quantum-Chemical Studies on the Relationship between Electronic and Antioxidant Properties. *Journal of Physics and Chemistry of Solids* **2020**, *140*. https://doi.org/10.1016/j.jpcs.2020.109362.
54. Pitucha, M.; Ramos, P.; Wojtunik-Kulesza, K.; Głogowska, A.; Stefańska, J.; Kowalczuk, D.; Monika, D.; Augustynowicz-Kopeć, E. Thermal Analysis, Antimicrobial and Antioxidant Studies of Thiosemicarbazone Derivatives. *Journal of Thermal Analysis and Calorimetry* **2023**, *148*, 4223–4234. https://doi.org/10.1007/s10973-023-12029-z.